Hindawi Publishing Corporation
Journal of Nanomaterials
Volume 2015, Article ID 275230, 8 pages
http://dx.doi.org/10.1155/2015/275230

Research Article

Fabrication and Characterization of Cellulose Acetate/Montmorillonite Composite Nanofibers by Electrospinning

Se Wook Kim,[1] Seong Ok Han,[1] I Na Sim,[1] Ja Young Cheon,[2] and Won Ho Park[2]

[1]*Energy Materials and Convergence Research Department, Korea Institute of Energy Research, 71-2 Jang-dong, Yuseong-gu, Daejeon 305-343, Republic of Korea*
[2]*Department of Advanced Organic Materials and Textile System Engineering, Chungnam National University, 220 Gung-dong, Yuseong-gu, Daejeon 305-764, Republic of Korea*

Correspondence should be addressed to Seong Ok Han; sohan@kier.re.kr and Won Ho Park; parkwh@cnu.ac.kr

Received 3 September 2014; Accepted 11 February 2015

Academic Editor: Lan Xu

Nanofibers composed of cellulose acetate (CA) and montmorillonite (MMT) were prepared by electrospinning method. MMT was first dispersed in water and mixed with an acetic acid solution of CA. The viscosity and conductivity of the CA/MMT solutions with different MMT contents were measured to compare with those of the CA solution. The CA/MMT solutions were electrospun to fabricate the CA/MMT composite nanofibers. The morphology, thermal stability, and crystalline and mechanical properties of the composite nanofibers were characterized by scanning electron microscopy (SEM), transmission electron microscopy (TEM), energy dispersive X-ray spectroscopy (EDX), thermogravimetric analysis (TGA), X-ray diffraction (XRD), and tensile test. The average diameters of the CA/MMT composite nanofibers obtained by electrospinning 18 wt% CA/MMT solutions in a mixed acetic acid/water (75/25, w/w) solvent ranged from 150~350 nm. The nanofiber diameter decreased with increasing MMT content. TEM indicated the coexistence of CA nanofibers. The CA/MMT composite nanofibers showed improved tensile strength compared to the CA nanofiber due to the physical protective barriers of the silicate clay layers. MMT could be incorporated into the CA nanofibers resulting in about 400% improvement in tensile strength for the CA sample containing 5 wt% MMT.

1. Introduction

Electrospinning is a unique technique for producing nonwoven fabrics of nanofibers, which exhibit high specific surface area and porosity on account of their potential applications, such as sensors [1, 2], filtration [3–5], membranes, tissue engineering, and drug delivery [6–9]. In addition, electrospinning is a good and effective method for fabricating micro- to nanoscale fibers from a variety of polymers, such as cellulose acetate [10], polystyrene [11], polybutadiene [12], and polycaprolactone [13]. In electrospinning, a high voltage (ca. 10–30 kV) that is sufficient to overcome the surface tension of a pendant drop of polymer solution is applied to a capillary containing polymer solution to induce the ejection of fine charged jets toward a target. These jets are stretched and elongated before they reach the target and are then dried and collected as an interconnected web of small fibers [14].

Cellulose is the most abundant natural polymeric material with a polyfunctional macromolecular structure and environmentally benign nature. Despite being characterized by its extensive linearity, good flexibility, excellent durability, biodegradability, chemical resistance, mechanical strength, nontoxicity, and low cost, cellulose suffers from a lack of solubility in most organic solvents due to its supramolecular architecture. However, one of its organic soluble derivatives, cellulose acetate (CA), carries all of the aforementioned remarkable features as well as good solubility in organic solvents, making it an excellent material for electrospinning [15]. The electrospinning of CA has been studied using various solvents [10, 16].

Functional nanomaterials, such as metal nanoparticles, carbon nanotubes, and nanoclays, can be incorporated into the electrospun CA nanofibers. The incorporation of functional nanomaterials into a CA nanofibrous structure is an attractive hybridization method, because nanomaterials distributed evenly in the CA nanofibrous structure can be used for novel specific applications. The CA nanocomposites reinforced with nanoclay (montmorillonite, MMT) can be quite promising due to the remarkable improvement in the material properties of polymer composites with only a low percentage of MMT added. The main advantages of these nanocomposites are the improvements in mechanical properties, reduced flammability, and superior barrier properties compared to polymers or conventional micro- and macrocomposites. Nanocomposites of CA and MMT have been prepared into film- or paper-shaped composite structures by conventional compounding methods, such as solution casting [16], melt processing [17], and dispersion method [18], and mechanical properties of CA/MMT composites have been further improved by the addition of compatibilizer or plasticizer [19, 20]. On the contrary, nanofiber-nanoclay composites of CA and MMT have unique advantages compared to conventional CA/MMT nanocomposites, because of higher surface area and biodegradability. However, there is no report on the electrospinning of CA nanofiber incorporated with MMT.

In this study, CA/MMT composite nanofibers were prepared by facile compounding and electrospinning. The morphological, thermal, structural, and mechanical properties of CA/MMT nanofibers were analyzed by scanning electron microscopy (SEM), transmission electron microscopy (TEM), thermogravimetric analysis (TGA), X-ray diffraction (XRD), and tensile test. In addition, the effect of electrospinning parameters on the distribution of MMT in the CA nanofibers was described.

2. Materials and Methods

2.1. Materials. Cellulose acetate (CA, acetyl content 39.8%, MW = 30,000 g/mol) was purchased from Aldrich Co., USA. Acetic acid (>99%) was purchased from DC chemical Pure Chemical Co., Korea. The clay (montmorillonite, MMT cloisite 93A) was supplied by Southern Clay Products Co., USA. Acetic acid and water were mixed to a weight ratio of 75 : 25. The resulting solution is abbreviated to acetic acid/water (75/25).

2.2. Preparation of CA/MMT Solution for Electrospinning. The CA and CA/MMT solutions were prepared using an ultrasonic treatment. MMT powders were dried at 80°C for 24 h under vacuum prior to use. For the CA solution, CA at a concentration of 18 wt% was dissolved in acetic acid/water (75/25) between 65°C and 75°C for 5 h. For the CA/MMT solutions, a predetermined amount of MMT was dispersed in water with constant stirring for one day after ultrasonication for 2 h. The CA/MMT solutions were compounded with a 1, 3, 5, 7, or 9 wt% of MMT and CA solution. The CA/MMT composites electrospun from these solutions are referred to as CA/MMT-1, CA/MMT-3, CA/MMT-5, CA/MMT-7, and CA/MMT-9, respectively.

2.3. Electrospinning of CA/MMT Nanofibers. Electrospinning was performed using a single syringe attached to a needle (ID = 0.84 mm), a ground electrode (d = 21.5 cm, aluminum sheet on a drum with a variable rotation speed), and high voltage supply (ChungPa EMT Co., Korea). Each solution was fed at a rate of 2 mL/h using a syringe pump and electrospun at a positive voltage of 27 kV. The tip-to-collector distance was 10 cm and all electrospinning procedures were carried out at 19°C.

2.4. Characterization of CA/MMT Solutions and Nanofibers. The viscosity and conductivity of the CA and CA/MMT solutions were determined using a Brookfield digital viscometer (Model-DV-prime) and a conductivity meter (Isteck model 455C) at 19°C, respectively. The thermal properties of the electrospun nanofibers were characterized by TGA (TGA Q 500, TA Instruments) at a heating rate of 10°C/min with purging nitrogen gas at 100 mL/min. The derivative thermogravimetric (DTG) curves were also recorded. The crystallinity of the CA and CA/MMT nanofibers was investigated by XRD (D/MAX-2500 diffractometer, Rich. Rigaku Co., Japan) with Cu-Kα radiation (100 mA, 40 kV). The tensile strength of the electrospun nanofibers was examined under tensile loading conditions using an Instron tensile testing machine (model 4467, Instron Co., USA) according to the ASTM D-638 method. The crosshead speed was 5 mm/min. At least twenty measurements were taken for each sample, and the results were averaged to obtain a mean value. The surface morphology of the CA and the CA/MMT nanofibers was characterized by SEM (S-4700, Hitachi, Japan) at an acceleration voltage of 15–25 kV. Prior to the measurement, the specimens were coated with Au to prevent surface charging. Field emission TEM (FE-TEM, FEI, Tecnai F30 Super-twin operated at an accelerating voltage of 200~300 kV with a Gatan imaging filter (GIF) model 2002) was performed to confirm existence of the MMT layers within the nanofibers that were directly electrospun onto carbon-coated TEM grid with a 300 mesh. The composition of the nanofibers was confirmed from the energy dispersive X-ray spectroscopy (EDAX, Genesis) spectrum and mapping images.

3. Results and Discussion

3.1. Characterization of CA Solution. Han et al. reported that CA nanofibers could be electrospun continuously using a mixed acetic acid/water solvent and the optimum concentration of CA for long uniform nanofibers was 17 wt% [10]. In this study, the viscosities of CA and CA/MMT-5 solutions were measured to determine the optimum concentration of CA solution and the effect of MMT addition on the CA solution for electrospinning. Figure 1 shows the viscosity of the CA and CA/MMT solutions with various CA concentrations in the range of 13~23 wt% in the acetic acid/water (75/25) solvent system. The viscosities of the CA and CA/MMT solutions were similar and the addition of 5 wt% MMT to CA solutions had little effect on the viscosity at CA solution concentrations < 18 wt%. The viscosity of CA and CA/MMT-5 increased relatively rapidly at CA concentrations > 18 wt%.

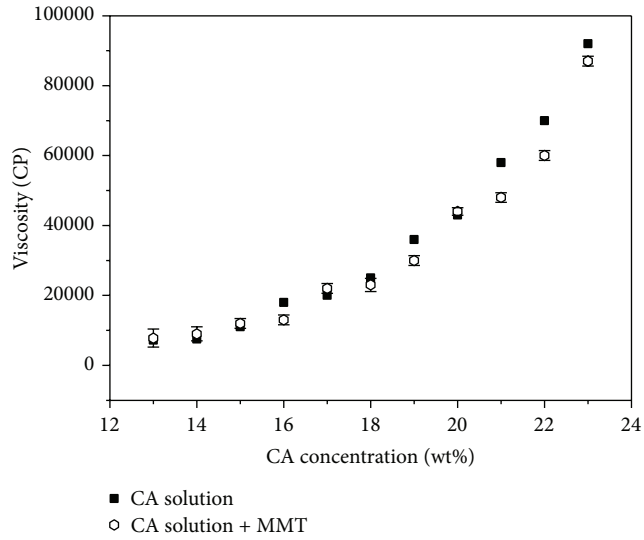

Figure 1: Changes in the viscosities according to the CA concentration.

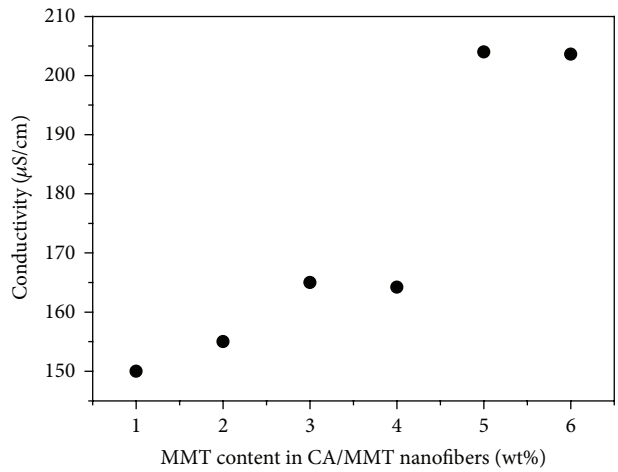

Figure 2: Changes in the conductivities with the MMT weight (1: pure CA, 2: CA/MMT1 wt%, 3: CA/MMT3 wt%, 4: CA/MMT5 wt%, 5: CA/MMT7 wt%, and 6: CA/MMT9 wt%).

The 18 wt% CA and CA/MMT-5 solutions were quite stable during the electrospinning process and could be electrospun continuously in a mixed acetic acid/water (75/25) solvent. Therefore, the CA nanofiber electrospun at 18 wt% was assigned as a standard nanofiber to examine the effect of MMT addition. CA and CA/MMT nanofibers with 18 wt% CA could be electrospun continuously using a mixed acetic acid/water (75/25) solvent.

Figure 2 shows the conductivity of the CA/MMT solutions with different MMT concentrations of 1, 3, 5, 7, and 9 wt% in the 18 wt% CA solution. The conductivity was relatively constant over the range of 1–5 wt% MMT but increased dramatically at MMT concentrations > 7 wt%. MMT addition at lower concentrations enhanced the mobility, but MMT concentrations > 7 wt% caused an increase in repulsion in the CA/MMT solution due to the charge of excess MMT. Some MMT did not interact with CA molecules and separately located in the solution at higher concentrations > 7 wt%, because there was lack of miscibility in those concentrations. The high conductivity due to excess MMT seemed to induce the formation of smaller nanofibers with some beads, as shown in Figures 3(e) and 3(f).

3.2. Morphology of CA and CA/MMT Nanofibers. Figure 3 shows the SEM images of the electrospun CA fiber and CA/MMT composite fibers with different MMT loadings prepared from 18 wt% CA in the acetic acid/water (75/25) solvent system. CA nanofibers were well electrospun and formed a fibrous web with diameters ranging from 150 to 350 nm. The diameter of the nanofibers was reduced by adding MMT. In case of CA/MMT-5, a relatively uniform nanoweb was obtained through the continuous electrospinning from the solution to the charged target wrapped with aluminum sheet. However, the diameters of the nanofibers electrospun

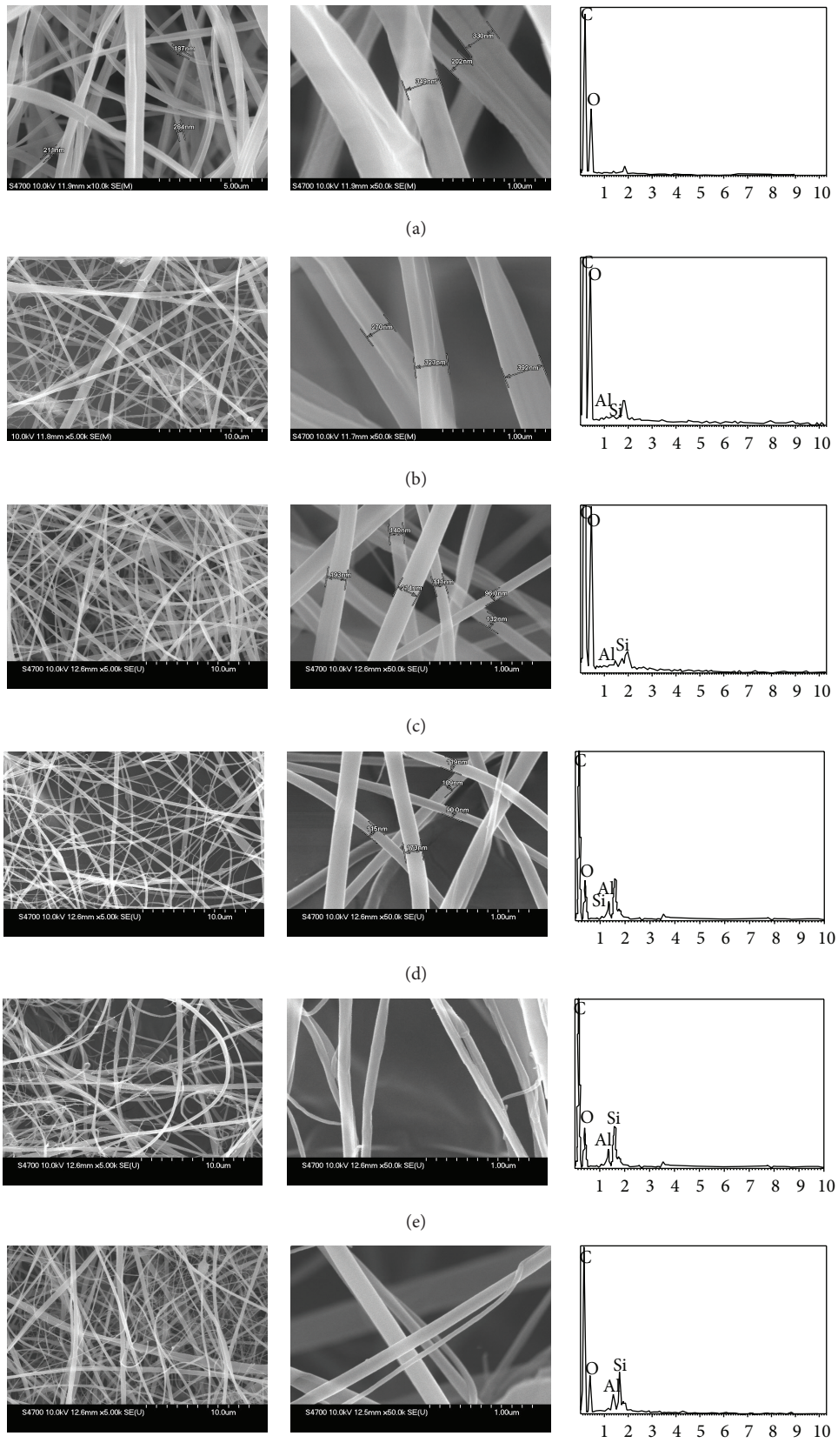

Figure 3: SEM images of (a) CA, (b) CA/MMT1 wt%, (c) CA/MMT3 wt%, (d) CA/MMT5 wt%, (e) CA/MMT7 wt%, and (f) CA/MMT9 wt%.

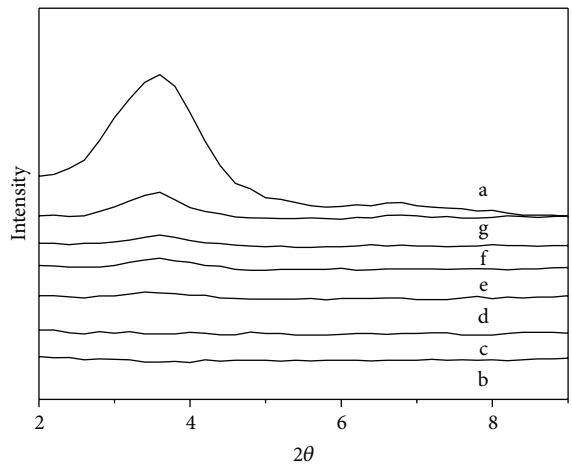

Figure 4: XRD patterns of CA nanofibers with various MMT contents (a, pure MMT; b, CA/MMT9 wt%; c, CA/MMT7 wt%; d, CA/MMT5 wt%; e, CA/MMT3 wt%; f, CA/MMT1 wt%; g, pure CA).

from higher MMT concentrations, such as CA/MMT-7 and CA/MMT-9, were decreased, but not uniform with increasing MMT concentration. An increase in the Si and Al peaks was observed with the addition of higher concentrations of MMT from the EDAX analysis of CA/MMT nanofibers. The addition of a quaternary ammonium salt of MMT increased the charge density in the ejected jets and imposed stronger elongation forces to the jets because of the self-repulsion of the excess charges under the electrostatic field, resulting in electrospun fibers with a substantially smaller diameter [19, 20]. As expected, the increase in the conductivity of CA/MMT with higher MMT concentrations caused a significant decrease in the diameter of the CA/MMT nanofibers.

The extent of MMT intercalation and dispersion can be usually obtained from the WAXS and TEM results [21]. Figure 4 shows the XRD patterns of MMT, CA, and CA/MMT nanofibers with different MMT contents. The patterns revealed changes in the interlayer distances. The CA nanofibers did not show any XRD, but MMT showed a (001) diffraction peak at 3.8° 2θ. This diffraction peak was not observed in the CA/MMT-1 and CA/MMT-3 samples, indicating that most of the MMT had been exfoliated and well-dispersed in the CA matrix. However, the CA/MMT-5, CA/MMT-7, and CA/MMT-9 samples showed a broad weak diffraction peak at 3.5° 2θ due to a small amount of intercalated MMT layers. This peak was shifted towards lower 2θ values (by 0.3 2θ), indicating that the polymer chains had diffused into the clay galleries, expanding the clay structure [22].

Figure 5 shows the TEM and EDX results of CA/MMT-5 that support MMT incorporation into CA fibers. The TEM image showed that the exfoliated MMT layers were distributed within the CA/MMT composite nanofibers. The EDX spectra recorded at two points identified C, Al, Si, and O in the CA/MMT composite nanofibers (right insets of (a)). A detail observation in scanning TEM (STEM) mode clearly showed that the MMT layers appeared to be incorporated into the CA/MMT composite nanofibers. The mapping data of the STEM image revealed that C element is a primary component of the CA/MMT composite nanofibers, and MMT layers composed of Al, Si, and O elements were evenly distributed in the CA nanofibers. These results were well consistent with previous reports [20].

Table 1: The residue and decomposition temperature at onset and 20% rate of pure MMT and nanofibers (pure CA, CA/MMT-1, CA/MMT-3, CA/MMT-5, CA/MMT-7, and CA/MMT-9).

Materials	T_d onset (°C)	T_d 20% (°C)	Residue at 500°C (%)
Pure CA	280	340	13
Pure MMT	280	380	65
CA/MMT-1	275	330	13
CA/MMT-3	275	325	14
CA/MMT-5	270	315	15
CA/MMT-7	270	310	17
CA/MMT-9	270	310	18

3.3. Thermal and Mechanical Properties of CA and CA/MMT Nanofibers. The thermal stability of the electrospun fibers was evaluated using TGA in a nitrogen atmosphere. Figure 6 shows the TGA curves of MMT, pure CA nanofiber, and CA/MMT composite nanofibers with different MMT loadings. Both the MMT and the CA nanofibers began to decompose at 280°C. However, they have single maximum decomposition temperatures of 390°C and 350°C, respectively (Samples a and b). In addition, the residues of MMT and CA nanofibers after thermal decomposition at 500°C were 65% and 13%, respectively (Table 1). However, the decomposition peaks for the CA/MMT composite nanofibers were divided into two peaks, at approximately 300°C and 350°C, as clearly seen from DTG curves. A higher concentration of MMT in the CA nanofiber induced a lower onset temperature of decomposition for CA/MMT composite nanofibers (Table 1). This is because the alkylammonium cations of MMT were thermally unstable and decomposed at lower temperatures. These aspects would reduce the thermal stability of CA nanofibers with the addition of MMT. However, the silicate clay layers could act as a superior insulator and mass-transport barrier and mitigate the escape of volatile products generated during thermal decomposition [23, 24].

Figure 7 shows the tensile strength of the CA/MMT nanofibers with different MMT concentrations. The tensile strength of the CA nanofibers increased with increasing MMT concentration reaching the highest tensile strength of 3.2 MPa (about 400% increase) at 5 wt% MMT. At higher MMT concentration (7 wt%), the tensile strength decreased abruptly to 1.5 MPa. The improvement in tensile strength was mainly due to reinforcing effect of MMT layers originated from the good dispersion of MMT layers in the CA fibrous matrix. However, some excess MMT seemed to be phase-separated and poorly dispersed in CA/MMT nanofibers at higher MMT concentration (7 wt%), whereas the exfoliated MMT layers were well-dispersed within CA/MMT nanofibers at 5 wt% MMT. The tensile strength of CA/MMT composite nanofibers was consistent with the results of XRD and EDX.

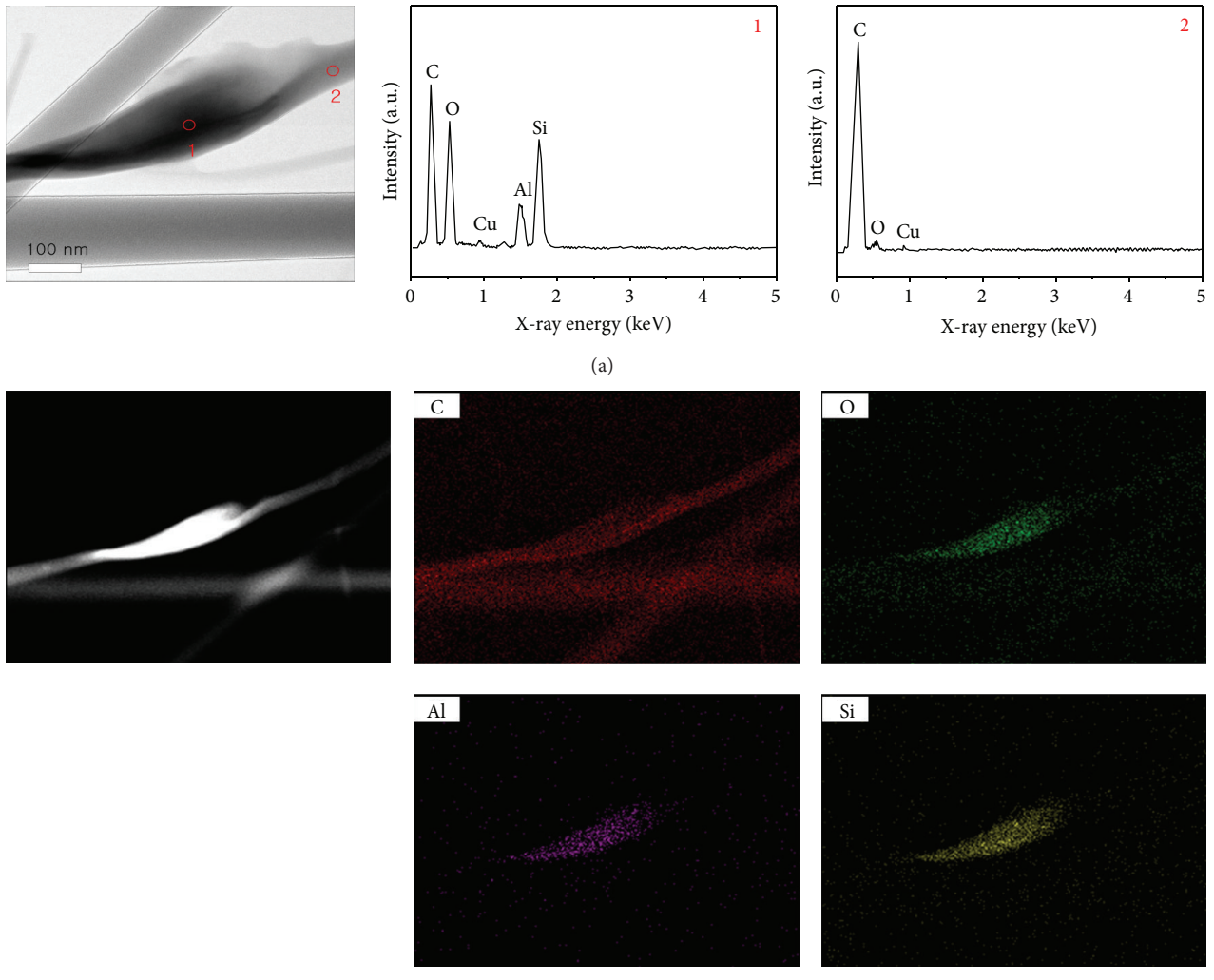

Figure 5: (a) TEM image and EDX spectra (right insets) of the CA/MMT nanofibers. (b) STEM image and mapping images clearly showed the existence of a MMT layer, composed of Al, Si, and O, within the CA/MMT nanofibers.

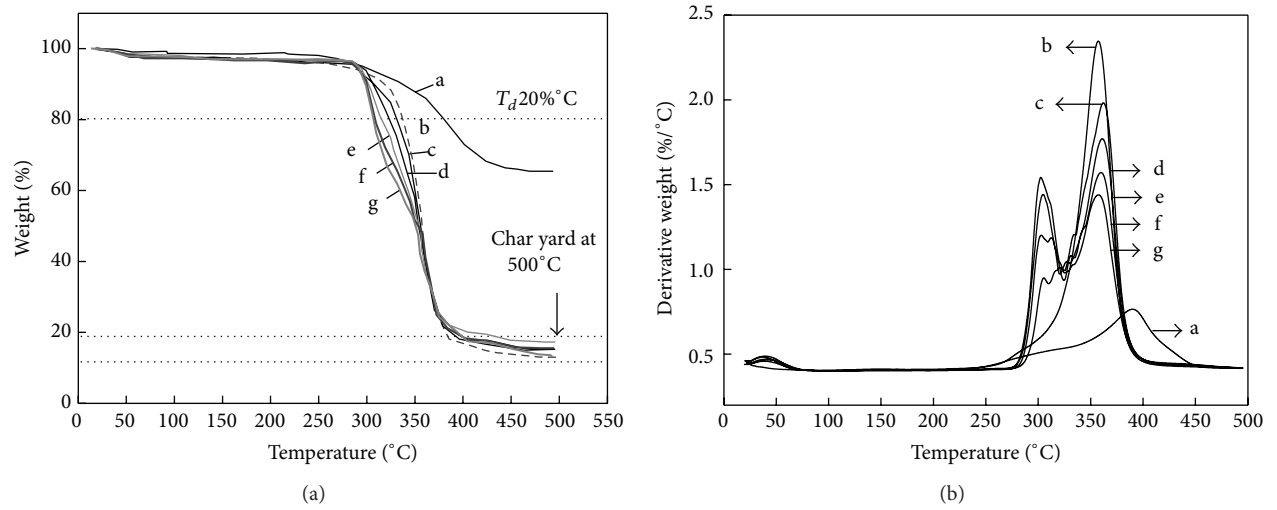

Figure 6: (a) TGA and (b) DTG thermograms showing the thermal stability of electrospun CA nanofiber and CA/MMT nanofiber (a, pure MMT; b, CA/MMT9 wt%; c, CA/MMT7 wt%; d, CA/MMT5 wt%; e, CA/MMT3 wt%; f, CA/MMT1 wt%; g, pure CA).

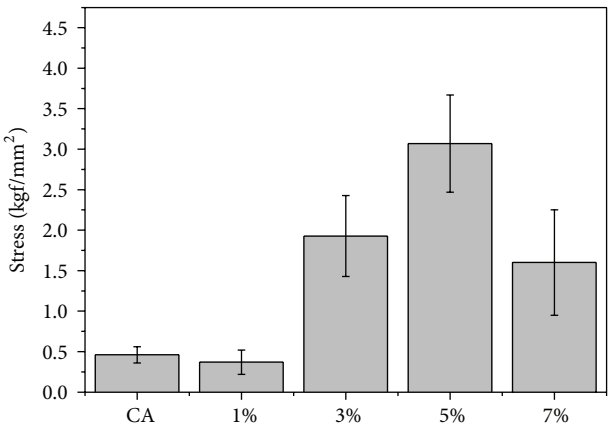

Figure 7: Tensile strength of CA, CA/MMT1 wt%, CA/MMT3 wt%, CA/MMT5 wt%, and CA/MMT7 wt% nanofibers.

4. Conclusions

The CA/MMT composite nanofibers were prepared using a facile compounding and electrospinning technique. The structures, thermal stability, and crystalline properties of the electrospun composite nanofibers were investigated. The average diameters of the CA/MMT nanofibers obtained by electrospinning 18 wt% CA/MMT solutions in a mixed acetic acid/water (75/25, w/w) solvent ranged from 150~350 nm. The nanofiber diameter decreased with increasing MMT content. TEM indicated the coexistence of CA nanofibers and MMT layers. The CA/MMT composite nanofibers showed improved tensile strength compared to the CA nanofiber due to the physical protective barriers of the silicate clay layers.

Conflict of Interests

The authors declare that there is no conflict of interests regarding the publication of this paper.

Acknowledgments

This study was supported financially by the Carbon Dioxide Reduction and Sequestration (CDRS) R&D Center (the 21st Century Frontier R&D Program) and by the Basic Science Research Program through the National Research Foundation of Korea (NRF), funded by the Ministry of Science, ICT & Future Planning (2012R1A1A2008761).

References

[1] Y. Xia, T. Fei, Y. He, R. Wang, F. Jiang, and T. Zhang, "Preparation and humidity sensing properties of $Ba_{0.8}Sr_{0.2}TiO_3$ nanofibers via electrospinning," *Materials Letters*, vol. 66, no. 1, pp. 19–21, 2012.

[2] S.-H. Choi, S.-J. Choi, B. K. Min, W. Y. Lee, J. S. Park, and I.-D. Kim, "Facile synthesis of p-type perovskite $SrTi_{0.65}Fe_{0.35}O_{3-\delta}$ nanofibers prepared by electrospinning and their oxygen-sensing properties," *Macromolecular Materials and Engineering*, vol. 298, no. 5, pp. 521–527, 2013.

[3] A. F. Lubambo, R. A. de Freitas, M.-R. Sierakowski et al., "Electrospinning of commercial guar-gum: effects of purification and filtration," *Carbohydrate Polymers*, vol. 93, no. 2, pp. 484–491, 2013.

[4] M. J. A. Shirazi, S. Bazgir, M. M. A. Shirazi, and S. Ramakrishna, "Coalescing filtration of oily wastewaters: characterization and application of thermal treated, electrospun polystyrene filters," *Desalination and Water Treatment*, vol. 51, no. 31–33, pp. 5974–5986, 2013.

[5] S. Adibzadeh, S. Bazgir, and A. A. Katbab, "Fabrication and characterization of chitosan/poly(vinyl alcohol) electrospun nanofibrous membranes containing silver nanoparticles for antibacterial water filtration," *Iranian Polymer Journal*, vol. 23, no. 8, pp. 645–654, 2014.

[6] H. Zhang, X. Jia, F. Han et al., "Dual-delivery of VEGF and PDGF by double-layered electrospun membranes for blood vessel regeneration," *Biomaterials*, vol. 34, no. 9, pp. 2202–2212, 2013.

[7] J. Jiang, J. Xie, B. Ma, D. E. Bartlett, A. Xu, and C. H. Wang, "Mussel-inspired protein-mediated surface functionalization of electrospun nanofibers for pH-responsive drug delivery," *Acta Biomaterialia*, vol. 10, no. 3, pp. 1324–1332, 2014.

[8] N. G. Rim, C. S. Shin, and H. Shin, "Current approaches to electrospun nanofibers for tissue engineering," *Biomedical Materials*, vol. 8, no. 1, Article ID 014102, 2013.

[9] S. Huang, X. Kang, Z. Cheng, P. Ma, Y. Jia, and J. Lin, "Electrospinning preparation and drug delivery properties of Eu^{3+}/Tb^{3+} doped mesoporous bioactive glass nanofibers," *Journal of Colloid and Interface Science*, vol. 387, no. 1, pp. 285–291, 2012.

[10] S. O. Han, J. H. Youk, K. D. Min, Y. O. Kang, and W. H. Park, "Electrospinning of cellulose acetate nanofibers using a mixed solvent of acetic acid/water: effects of solvent composition on the fiber diameter," *Materials Letters*, vol. 62, no. 4-5, pp. 759–762, 2008.

[11] J. Lin, B. Ding, Y. Jianyong, and Y. Hsieh, "Direct fabrication of highly nanoporous polystyrene fibers via electrospinning," *ACS Applied Materials and Interfaces*, vol. 2, no. 2, pp. 521–528, 2010.

[12] M. Tian, Q. Hu, H. Wu, L. Zhang, H. Fong, and L. Zhang, "Formation and morphological stability of polybutadiene rubber fibers prepared through combination of electrospinning and in-situ photo-crosslinking," *Materials Letters*, vol. 65, no. 19-20, pp. 3076–3079, 2011.

[13] J. Johnson, A. Niehaus, S. Nichols et al., "Electrospun PCL in vitro: a microstructural basis for mechanical property changes," *Journal of Biomaterials Science*, vol. 20, no. 4, pp. 467–481, 2009.

[14] G. E. Wnek, M. E. Carr, D. G. Simpson, and G. L. Bowlin, "Electrospinning of nanofiber fibrinogen structures," *Nano Letters*, vol. 3, no. 2, pp. 213–216, 2003.

[15] Y. Nishio, "Material functionalization of cellulose and related polysaccharides via diverse microcompositions," *Advances in Polymer Science*, vol. 205, no. 1, pp. 97–151, 2006.

[16] R. Konwarh, N. Karak, and M. Misra, "Electrospun cellulose acetate nanofibers: the present status and gamut of biotechnological applications," *Biotechnology Advances*, vol. 31, no. 4, pp. 421–437, 2013.

[17] H. M. Park, X. Liang, A. K. Mohanty, M. Misra, and L. T. Drzal, "Effect of compatibilizer on nanostructure of the biodegradable cellulose acetate/organoclay nanocomposites," *Macromolecules*, vol. 37, no. 24, pp. 9076–9082, 2004.

[18] H.-M. Park, M. Misra, L. T. Drzal, and A. K. Mohanty, "'Green' nanocomposites from cellulose acetate bioplastic and clay: effect of eco-friendly triethyl citrate plasticizer," *Biomacromolecules*, vol. 5, no. 6, pp. 2281–2288, 2004.

[19] Y. Cai, F. Huang, Q. Wei et al., "Structure, morphology, thermal stability and carbonization mechanism studies of electrospun PA6/Fe-OMT nanocomposite fibers," *Polymer Degradation and Stability*, vol. 93, no. 12, pp. 2180–2185, 2008.

[20] M. Manitiu, S. Horsch, E. Gulari, and R. M. Kannan, "Role of polymer-clay interactions and nano-clay dispersion on the viscoelastic response of supercritical CO_2 dispersed polyvinylmethylether (PVME)-Clay nanocomposites," *Polymer*, vol. 50, no. 15, pp. 3786–3796, 2009.

[21] M. Hassan-Nejad, J. Ganster, A. Bohn, M. Pinnow, and B. Volkert, "Bio-based nanocomposites of cellulose acetate and nano-clay with superior mechanical properties," *Macromolecular Symposia*, vol. 280, no. 1, pp. 123–129, 2009.

[22] Y. Ji, B. Li, S. Ge, J. C. Sokolov, and M. H. Rafailovich, "Structure and nanomechanical characterization of electrospun PS/clay nanocomposite fibers," *Langmuir*, vol. 22, no. 3, pp. 1321–1328, 2006.

[23] J. Zhang and C. A. Wilkie, "Fire retardancy of polyethylene-alumina trihydrate containing clay as a synergist," *Polymers for Advanced Technologies*, vol. 16, no. 7, pp. 549–553, 2005.

[24] J. Zhu, A. B. Morgan, F. J. Lamelas, and C. A. Wilkie, "Fire properties of polystyrene-clay nanocomposites," *Chemistry of Materials*, vol. 13, no. 10, pp. 3774–3780, 2001.